APEM journal
Advances in Production Engineering & Management
Volume 17 | Number 2 | June 2022 | pp 141–151
https://doi.org/10.14743/apem2022.2.426
ISSN 1854-6250
Journal home: apem-journal.org
Original scientific paper

A method for prediction of *S-N* curve of spot-welded joints based on numerical simulation

Yang, L.[a], Yang, B.[a], Yang, G.W.[a,*], Xiao, S.N.[a], Zhu, T.[a], Wang, F.[a]

[a]State Key Laboratory of Traction Power, Southwest Jiaotong University, Chengdu, P.R. China

ABSTRACT

Currently, $\triangle F$-N curves are often used to predict the fatigue lives of spot-welded joints, but the method for obtaining these $\triangle F$-N curves is time-consuming, laborious, and non-universal. Tensile-shear fatigue tests were performed to obtain the fatigue lives and the corresponding normalized *S-N* curves of spot-welded joints. Subsequently, the force acting at the spot-welded joints was obtained by extracting the force and moment of the beam element in the shell-element-based finite element model, and the equivalent structural stress at the spot-welded joint was obtained based on the equivalent structural stress method. Finally, the *S-N* curves of the spot-welded joints were fitted using the least-squares method. A comparison of the *S-N* curves of the spot-welded joints with those of different materials revealed that the material type had a significant influence on the *S-N* curve. To avoid this influence, a method for predicting the *S-N* curve of the spot-welded joints was proposed based on the relationship between the ratio of the tensile strength and that of the fatigue limit of each material. This research provides guidance for predicting the fatigue life of spot-welded joints in engineering applications.

ARTICLE INFO

Keywords:
Spot-welded joints;
Simulation;
Numerical simulation;
Finite element methods (FEM);
S-N curve;
Prediction method;
Equivalent structural stress

**Corresponding author:*
gwyang@home.swjtu.edu.cn
(Yang, G.W.)

Article history:
Received 4 April 2022
Revised 16 August 2022
Accepted 20 August 2022

1. Introduction

Spot-welded structures are widely used in modern industrial production owing to their advantages of light weight, stable performance, and high automated production efficiency. This is an important connection mode in the mechanical manufacturing process [1]. Spot welding is mainly used in the fields of automobile manufacturing, rail-vehicle manufacturing, aerospace, and ship building, especially in automobile bodies and stainless-steel bodies of rail vehicles. According to statistics, a stainless-steel body of rail vehicles usually has up to 50000 spot-welded joints, and an automotive body has approximately 4000-6000 spot-welded joints [2].

As the spot-welding nugget is located between two relatively close plates and fatigue cracks often appear on the inner side of the plate, it becomes difficult to monitor the crack length and depth and perform non-destructive inspection [3-6]. Spot-welding fatigue-assessment methods mainly include the load-life, nominal stress, hot-spot stress, local, notch stress, fracture mechanics, and equivalent structural stress methods. At present, the load-life method specified in the standards ISO 14324-2003 [7], NF A89-571-2004 [8], JIS Z3138-1989 [9], KS B 0528-2001 [10], and GB/T 15111-1994 [11] are still used to predict the fatigue life of spot-welded joints. Howev-

er, the $\triangle F$-N (load-amplitude-life) curves corresponding to different types of spot-welded joints in these standards are limited, and it is impossible to establish $\triangle F$-N curves for individual spot-welding structures; furthermore, the load-life method is an approximate estimation method [12]. Therefore, the limitations of the load-life method are evident. In addition, other spot-welding fatigue assessment methods have limitations, such as high sensitivity to finite element meshes and a small application range, while the equivalent structural stress method has been widely used owing to its insensitivity to meshes.

Current spot-welding fatigue-life prediction methods based on equivalent structural stress include the Radaj [13], Rupp [14], Sheppard [15], Kang [16], and Dong methods [17]. In the early stages of fatigue research of spot-welded joints, Radaj [13] derived the formula for the maximum equivalent structural stress at the edge of a weld nugget. Based on the Roark stress-strain formula, Rupp [14] predicted the fatigue lives of spot-welded joints using the structural stress and verified the accuracy of the structural stress via tests. Sheppard [15] calculated the equivalent structural stress using the spot-welding finite element model and evaluated the fatigue lives of spot-welded joints according to the relationship between the structural stress and fatigue life. Kang [16] substituted the stress components in the von Mises equation with the local structural stresses in the vicinity of the spot weld and used the forces and moments that were determined via finite element analysis to calculate the structural stresses at the edges of the weld nugget in each sheet. Through a finite element simulation, Dong [17] transformed the nodal forces and moments at the edge of the spot-welding nugget into the linear membrane stress and bending stress and proposed a structural-stress calculation method that was insensitive to meshes. Subsequently, Yan [18] combined the Dong and Rupp methods and proposed a new fatigue characteristic parameter and simplified structural stress of the spot welding. Subsequently, the author determined the correlations of the spot-welding fatigue characteristic parameters of the Rupp, Kang, Dong, and Sheppard structure stresses on the fatigue performance of single and double spot welding [19]. Wu [20] used the classical, nonlinear generalized reduced-gradient algorithm to propose a process for optimizing the empirical parameter terms in the Rupp structural stress formula. The optimized Rupp structural-stress formula can effectively correlate the fatigue lives of spot-welded joints of various geometric sizes.

The aforementioned studies have made significant contributions to the fatigue-life evaluation method, equivalent-structural-stress calculation method, finite element simulation method, fatigue characteristic parameters, and fatigue influence parameters of spot welding. However, there is insufficient research on the normalized-spot-welding S-N curve and the method for predicting the S-N curve.

Different from the above studies, in this study, the quasi-static failure loads of spot-welded joints of different materials were obtained by carrying out quasi-static tensile tests. Based on the quasi-static failure loads, the load levels of tensile-shear fatigue tests were determined, and the fatigue lives of the spot-welded joints were obtained via tensile-shear fatigue tests. The equivalent structural stresses of the spot-welded joints were obtained based on the Rupp equivalent structural stress method, and the S-N curves of the spot-welded joints were fitted based on the least-squares method. Finally, based on the influence of the material on the S-N curve, a method for predicting the S-N curve of spot-welded joints was proposed, which provides a useful reference for engineering applications.

2. Materials, methods, and experimental testing

In this study, tensile-shear fatigue tests were performed on spot-welded specimens to study the fatigue lives of spot-welded joints. Because the process of welding the stainless-steel body of rail vehicles often comprises the use of spot-welded joints, the SUS301L stainless steel commonly used in the stainless-steel body was selected as the specimen material. To avoid eccentricity in the fatigue test process of the plate welding specimens of various thicknesses, the upper and lower auxiliary plates were welded onto the plate to ensure that the spot-welded joint was stressed uniformly. The parameters of the spot-welded specimens are listed in Table 1, and the structural diagram is presented in Fig. 1.

Table 1 Parameters of spot-welded specimens

Type	Upper plate		Lower plate				Weld nugget diameter (mm)	Load ratio
	Material	Thickness (mm)	Material	Thickness (mm)	Yield strength (MPa)	Tensile strength (MPa)		
A_1	SUS301L_ 1/8H	1.5	SUS301L_ 1/8H	2	380	690	6	0.1
A_2	SUS301L_ 1/8H	2	SUS301L_ 1/8H	2	380	690	7	0.1
B	SUS301L_ 1/16H	1.5	SUS301L_ 1/16H	3	450	790	6	0.1
C	SUS301L_ 1/4H	2	SUS301L_ 1/4H	2	515	860	7	0.1

Note: Type-A_1 and Type-A_2 comprise the same material, and only their sizes are different. Type-A is the name used to indicate Type-A_1 and Type-A_2.

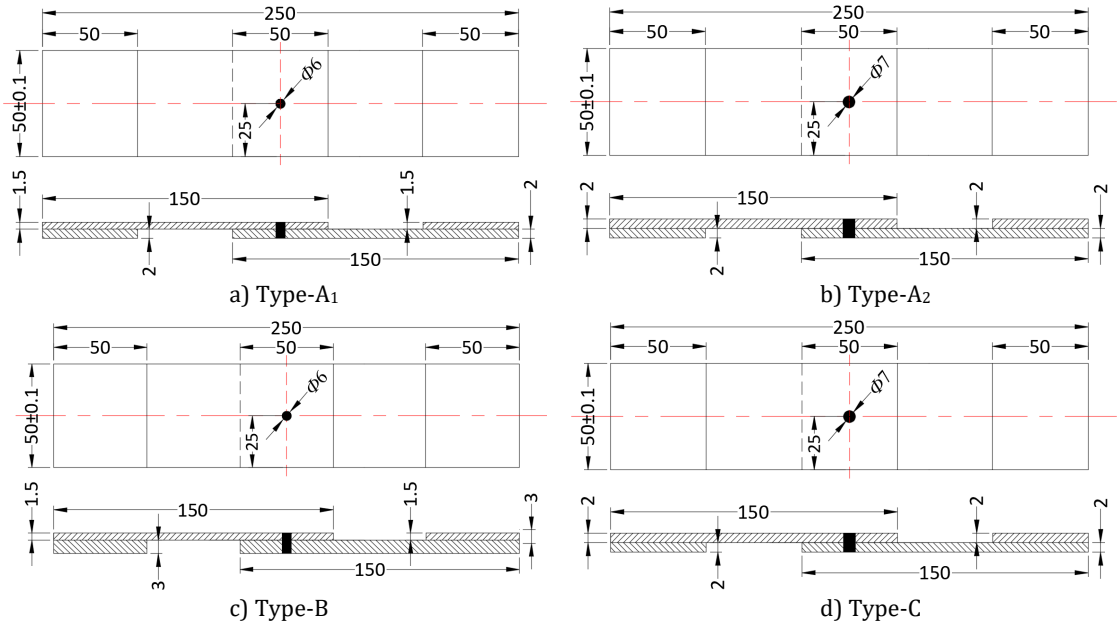

Fig. 1 The structural diagram of spot-welded specimens

Table 2 Quasi-static tensile test results of spot-welded specimens

Specimen serial number	Failure load F (kN)			
	Type-A_1	Type-A_2	Type-B	Type-C
1	20.66	23.42	26.24	40.53
2	21.01	22.98	26.77	41.61
3	20.50	23.57	26.84	42.01
4	23.31	23.29	26.93	41.98
5	22.26	22.75	26.72	41.74
Average failure load $\overline{F}$	21.548	23.202	26.70	41.574

First, the specimens presented in Fig. 1 were installed on a hydraulic universal testing machine (WE-30) for the quasi-static tensile test to determine the failure load of the spot-welded specimens. The test results are listed in Table 2.

Based on the average failure load $\overline{F}$ in Table 2, the tensile-shear fatigue tests were then performed under four sets of load levels (multiples of $\overline{F}$) on a PLG-20C high-frequency tension-and-compression fatigue-testing machine for each spot-welded specimen. The group and the ladder test methods were used, the load form was an equal-amplitude sinusoidal curve, and the load ratio was 0.1 ($F_{\min}/F_{\max}$). The loading frequency gradually decreased with the crack propagation in the specimens, and the frequency range was 50-1000 Hz. While considering the fatigue fracture of the spot-welded specimens as the failure criterion, the fatigue lives of the spot-welded specimens were obtained, as shown in Table 3.

Table 3 Tensile-shear fatigue test loads and fatigue lives of spot-welded specimens

Type-A_1		Type-A_2		Type-B		Type-C	
F_{max} (kN)	N (cycle)	F_{max} (kN)	N (cycle)	F_{max} (kN)	N (cycle)	F_{max} (kN)	N (cycle)
3.2322 kN (15 % $\bar{F}$)	340800	4.6404 kN (20 % $\bar{F}$)	186700	4.005 kN (15 % $\bar{F}$)	358500	4.1574 kN (10 % $\bar{F}$)	373750
	495300		202600		400600		406659
	671700		209000		418209		419313
	997900		307843		433200		426488
	1085900		522400		537000		497444
4.3096 kN (20 % $\bar{F}$)	150900	6.9606 kN (30 % $\bar{F}$)	36500	6.675 kN (25 % $\bar{F}$)	92100	8.3148 kN (20 % $\bar{F}$)	58208
	199600		38300		97100		59175
	205700		42900		105700		81142
	218300		53500		120500		152638
	356100		55300		134700		162663
5.387 kN (25 % $\bar{F}$)	35100	9.2808 kN (40 % $\bar{F}$)	15300	9.345 kN (35 % $\bar{F}$)	32100	12.4722 kN (30 % $\bar{F}$)	14028
	62800		16700		36600		14133
	85500		22200		40500		14439
	91300		22300		57200		15123
	93300		25300		58800		15476
6.4644 kN (30 % $\bar{F}$)	22300	11.6010 kN (50 % $\bar{F}$)	4700	12.015 kN (45 % $\bar{F}$)	14200	16.6296 kN (40 % $\bar{F}$)	4986
	28300		7600		16100		5118
	37800		8400		22400		5366
	46900		9000		23100		5439
	50700		10600		28000		5817

The $\triangle F$-N curves of the spot-welded specimens were obtained according to the test loads and tensile-shear fatigue lives of the specimens, as shown in Fig. 2. It can be observed that the overall dispersion of the data points was relatively high, and the correlations between the $\triangle F$-N curves for each material were weak. It was found that the correlation between the load amplitude $\triangle F$ and fatigue life N of the spot-welded joint was weak, and the $\triangle F$-N curves fitted appropriately only for the spot-welded joints of the same material. When predicting the fatigue lives of the spot-welded joints of different materials, fatigue tests were performed for each structure. This is time-consuming and laborious. Furthermore, the selection process also becomes cumbersome when too many curves are considered. Therefore, it is of greater engineering significance to plot the normalized S-N curves of spot-welded joints suitable for different steels and different weld sizes.

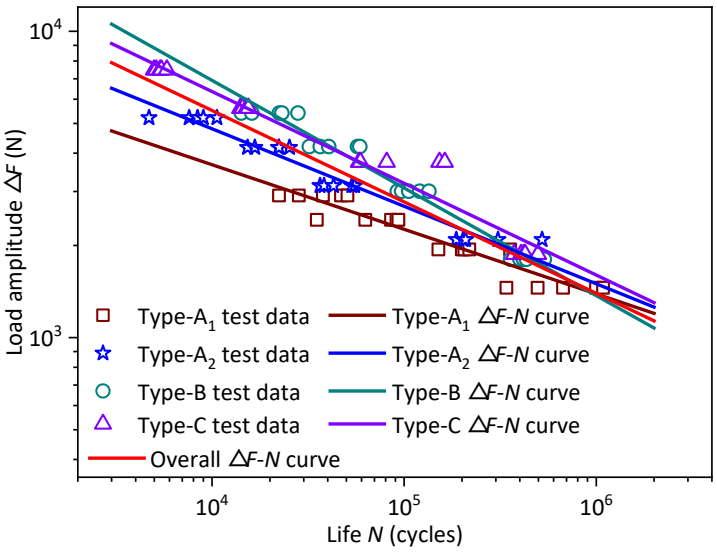

Fig. 2 $\triangle F$-N curves

3. Structural-stress calculation method

3.1 Structural-stress calculation model

To fit the *S-N* curve, it was necessary to obtain the structural stress (S) of the spot-welded joints. The spot-welding equivalent structural stress proposed by Rupp based on Roark's stress-strain formula is widely used in the fatigue-strength evaluation of spot-welded joints; its equivalent structural stress calculation model is presented in Fig. 3.

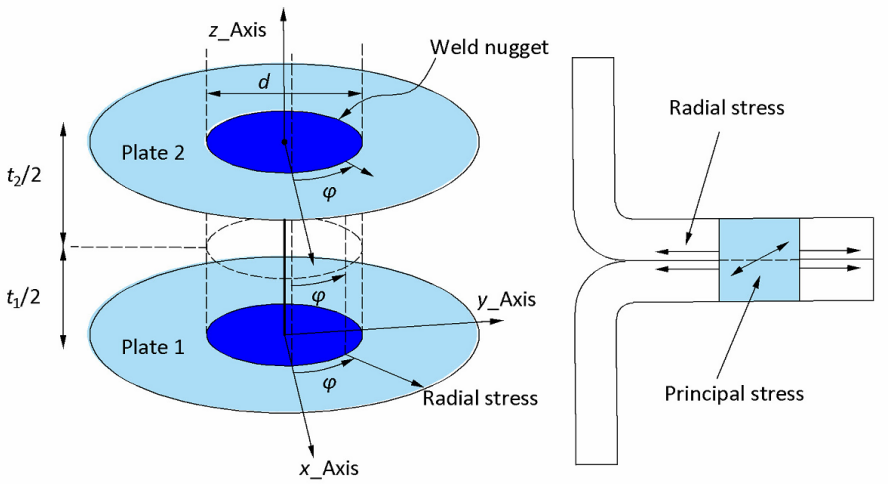

Fig. 3 Method for calculating equivalent-structural-stress of spot-welded joints

The plate thickness of the spot-welded joint in this study satisfied the relation $d > 3.5\sqrt{t}$ (d is the diameter of the weld nugget, t is the thickness of sheet). According to the structural-stress calculation model, the equivalent structural stress of a spot-welded joint was obtained, as shown in Eqs. 1 to 7, respectively [14].

$$\sigma_{v1} = -\sigma_{\max}(F_{x1})\cos\varphi - \sigma_{\max}(F_{y1})\sin\varphi + \sigma_{\max}(F_{z1}) + \sigma_{\max}(M_{x1})\sin\varphi - \sigma_{\max}(M_{y1})\cos\varphi \quad (1)$$

where

$$\sigma_{\max}(F_{x1}) = \frac{F_{x1}}{\pi d t_1} \quad (2)$$

$$\sigma_{\max}(F_{y1}) = \frac{F_{y1}}{\pi d t_1} \quad (3)$$

$$\sigma_{\max}(M_{x1}) = K_1\left(\frac{1.872M_{x1}}{dt_1^2}\right) \quad (4)$$

$$\sigma_{\max}(M_{y1}) = K_1\left(\frac{1.872M_{y1}}{dt_1^2}\right) \quad (5)$$

where t_1 is the thickness of sheet 1, $K_1 = 0.6\sqrt{t_1}$ is an empirical correction factor, and φ is the radial stress angle.

When the axial force on the weld nugget is a tensile force, it results in fatigue failure, and the influence of the axial force should be considered, that is, when $F_{z1} > 0$:

$$\sigma(F_{z1}) = K_1\left(\frac{1.774F_{z1}}{t_1^2}\right) \quad (6)$$

When the axial force on the weld nugget is the result of a pressure, fatigue does not occur. At this time, the effect of the axial force is ignored, that is, when $F_{z1} \leq 0$:

$$\sigma(F_{z1}) = 0 \quad (7)$$

3.2 Equivalent structural stress calculation

To obtain the force and moment at the spot welding, a finite element model of the spot-welded joint was established in the software HyperMesh, wherein the base metal was simulated as the shell element and the weld nugget was simulated as the CBAR element. The weld nugget center nodes of the upper-plate and lower-plate nuggets were connected using a CBAR element. The mesh size of the model was 2 mm, and the load and boundary conditions were consistent with

those of the test. One end of the specimen was fully constrained, the other end was connected to the rbe2 rigid elements, and the specimen was unconstrained in the direction of the load. The time of finite element model simulation was 38 s, and the required storage space was 8.04 MB. The spot-welded shell-element-based finite element model is presented in Fig. 4. This finite element model can accurately simulate the actual stress of the spot welding and easily obtain the stress of the spot-welded structure [2, 19, 21].

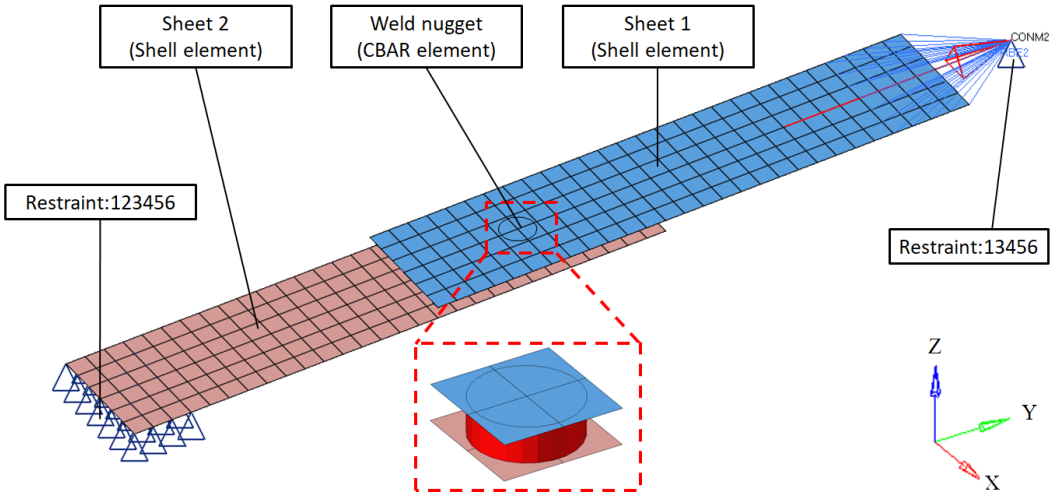

Fig. 4 Spot-welded shell-element-based finite element model

In the finite element simulation, first, the maximum and minimum loading forces F_{max} and F_{min}, respectively, of the different types of spot-welded specimens were applied to the finite element models. Then, the software NASTRAN was used to calculate the force and moment of the beam element nodes of the finite element models. Finally, the force and moment of the beam element nodes were introduced into Eqs. 1 to 7 to obtain the equivalent structural stresses of the spot-welded joints under tensile-shear loads. The calculation process is presented in Fig. 5 (A and B indicate the nodes at each end of the beam element).

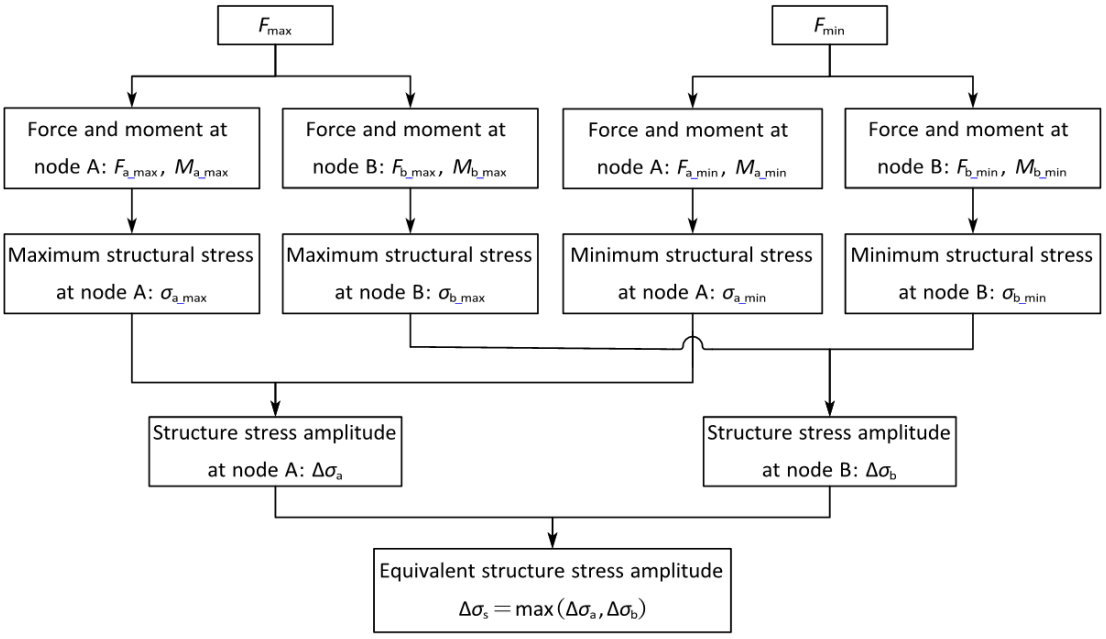

Fig. 5 Equivalent structural stress calculation process [22]

On considering the Type-B specimen, with F_{max} = 6.675 kN, as an example, according to the calculation process shown in Fig. 5, the force and moment of the beam-element nodes in the model and the equivalent-structural-stress amplitude of the spot-welded joint were obtained, as shown in Table 4.

Table 4 Force and moment of beam element nodes in the model and the equivalent-structural-stress amplitude of spot-welded joint

Nodes	Force and moment	F_{max} = 6675 N	F_{min} = 667.5 N	σ_{a_max}, σ_{b_max} (MPa)	σ_{a_min}, σ_{b_min} (MPa)	$\triangle\sigma_a$, $\triangle\sigma_b$ (MPa)	$\triangle\sigma_s$ (MPa)
Node A	M1 (N·mm)	-11490	-1149	549.184	54.918	494.266	580.166
	M2 (N·mm)	-2.929e-10	-2.884e-11				
	Shear1 (N)	-6675	-667.5				
	Shear2 (N)	-4.897e-11	-4.608e-12				
	Axial (N)	85.4	8.54				
	Torque (N·mm)	9.185e-15	8.526e-16				
Node B	M1 (N·mm)	3532	353.2	644.629	64.463	580.166	
	M2 (N·mm)	-1.827e-10	-1.847e-11				
	Shear1 (N)	-6675	-667.5				
	Shear2 (N)	-4.897e-11	-4.608e-12				
	Axial (N)	85.4	8.54				
	Torque (N·mm)	9.185e-15	8.526e-16				

4. *S-N* Curve and prediction method

4.1 Fitting *S-N* curve

The test data were fitted in a double-logarithmic coordinate system using the least-squares method by plotting the equivalent-structural-stress amplitude $\triangle\sigma_s$ along the ordinate and the fatigue life *N* along the abscissa, and the *S-N* curves of the spot-welded joints of the same material and of different materials were obtained as shown in Fig. 6.

In the processing of the fatigue test data, five times the lifespan (hereinafter referred to as "5×lifespan") is typically used to evaluate the *S-N* curve. If the data points are within the 5×lifespan, the *S-N* curve is considered to have a high correlation [2, 20, 22, 23]. It can be observed from Fig. 6 that all the spot-welding data points of the same material were within the 5×lifespan, the data points were relatively compact, and the squared correlation coefficient (R^2) of the *S-N* curves were greater than 0.8769; however, the spot-welding data points in the case of different materials were more dispersive, and R^2 was only 0.8667 in the *S-N* curve. Thus, the *S-N* curve of the spot welding of the same material had a higher correlation and a better fitting effect. The dispersion of the spot-welding data points for different materials resulted in a weak correlation of the overall *S-N* curve with R^2 of only 0.8742. It can be observed that the material had a significant influence on the *S-N* curve; therefore, the influence of the material cannot be ignored in the fatigue analysis of the spot-welded joints. It is necessary to distinguish the materials of spot-welded joints for the fatigue evaluation.

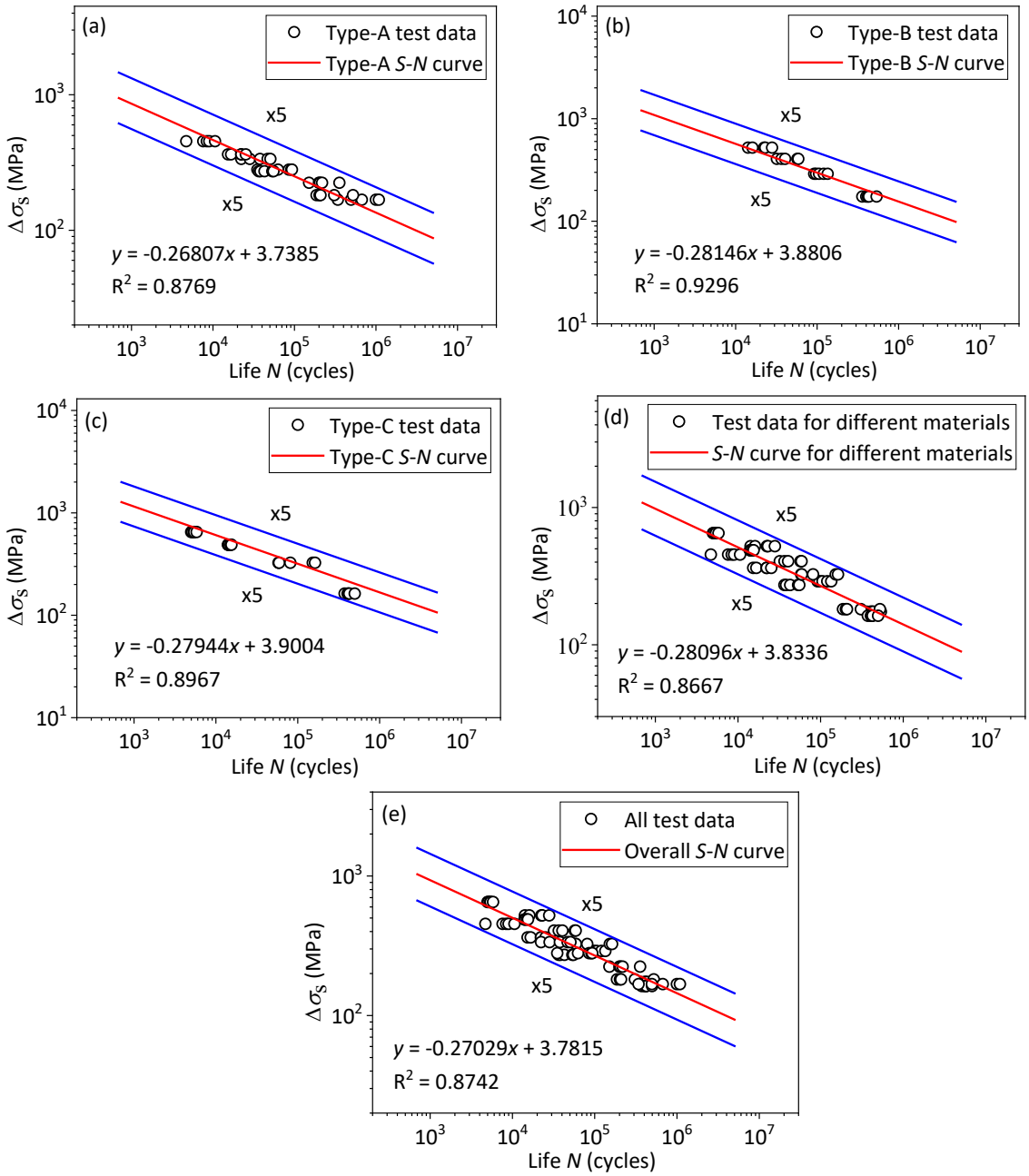

Fig. 6 *S-N* curves of spot-welded joints

4.2 *S-N* curve prediction method

The standard-power-function expression of the *S-N* curve is shown in Eq. 8, and all the spot-welding test fatigue lives N can be equivalent to the fatigue life N_e when the fatigue limit is 5e6 cycles as shown in Eq. 8 [24] and the equivalent equation is given by Eq. 9.

$$S^m N = \mathrm{C} \tag{8}$$

where m and C are parameters related to the material properties, specimen form, stress ratio, and loading mode, respectively.

$$N_e = N(\frac{S}{S_e})^m \tag{9}$$

where S_e is the stress amplitude corresponding to the *S-N* curve of the spot welding when N is 5e6 cycles.

The equivalent *S-N* curves are presented in Fig. 7, and it can be observed that the *S-N* curves of the spot-welded joints of all the materials after equivalence are almost parallel. The slopes and relative deviations of the *S-N* curves of the spot-welded joints are listed in Table 5. It can be

observed that the relative deviations of all the slopes are within 5 %. Within the acceptable error range, the *S-N* curves of the spot-welded joints of various materials were considered to be parallel. This indicates that the ratio of fatigue limit or that of the fatigue strength under different cycles of spot welding is a constant value, and the spot-welding *S-N* curve of one material can be derived from that of another material.

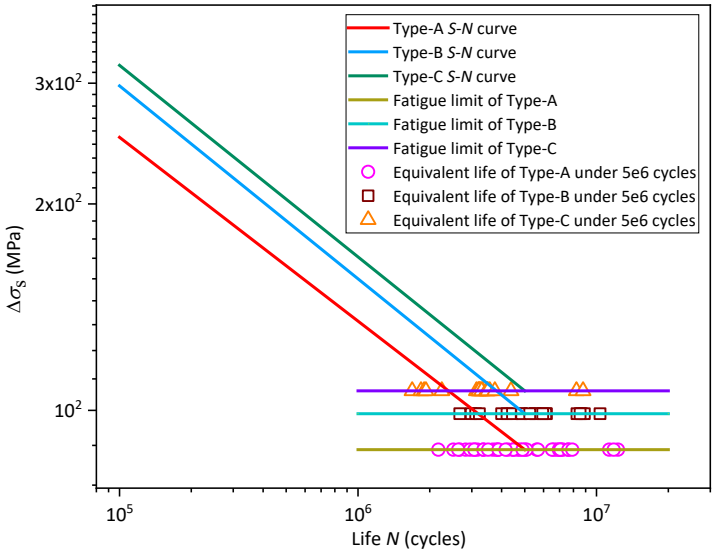

Fig. 7 The equivalent *S-N* curves of spot-welded joints

Because the fatigue limit of the material has a good correlation with the tensile strength [25], the tensile strength of the spot-welded joint material was compared with the fatigue limit, and the results are shown in Table 6. It can be observed that the ratio of the tensile strength of each material is very close to that of the fatigue limit, and the ratio deviation is within 3 %. This shows that the spot-welding *S-N* curve of other materials can be derived from the known spot-welding *S-N* curve of one material according to the ratio relationship of the tensile strength.

Table 5 Slopes and relative deviations of *S-N* curves of spot-welded joints

Item	Spot welding type			Slope relative deviation (%)		
	Type-A	Type-B	Type-C	Type-A versus Type-B	Type-A versus Type-C	Type-B versus Type-C
Slope of *S-N* curve	-0.26807	-0.28146	-0.27944	4.995	4.241	0.718

Table 6 Relationship between tensile strength of spot-welded joint material and *S-N* curve

Item	Type-A	Type-B	Type-C	Ratio of Type-A to Type-B	Ratio of Type-A to Type-C	Ratio of Type-B to Type-C
Tensile strength, MPa	690	790	860	0.873	0.802	0.919
Fatigue limit, MPa	87.641	98.880	106.768	0.886	0.821	0.926
Deviation (%)	/	/	/	1.458	2.258	0.812

According to the ratio relationship of the tensile strength of spot-welding materials, the spot-welding *S-N* curve of other materials was derived from the known spot-welding *S-N* curve of one material, as shown in Table 7. It can be observed that the derived fatigue limit of the spot welding was very close to the fatigue limit fitted according to the test data, and the corresponding error was within 3 %. Therefore, according to the ratio relationship of the tensile strength of the spot-welding materials, the spot-welding *S-N* curve of other materials can be predicted relatively accurately from the known spot-welding *S-N* curve of one material. In engineering applications, it is not necessary to perform tests on spot-welded joints of each material individually. Using the *S-N*-curve prediction method, the predicted *S-N* curves of other materials can be obtained, which is timesaving, labor-saving, and more universal and provides references for the design of spot-welding structures and life predictions in engineering applications.

Table 7 Spot welding *S-N* curves were derived according to the ratio relationship of the tensile strength of spot-welding materials

Item	Type-B derives Type-A	Type-C derives Type-A	Type-A derives Type-B	Type-C derives Type-B	Type-A derives Type-C	Type-B derives Type-C
Derived *S-N* curves	y = -0.28146x + 3.8218	y = -0.27944x + 3.8048	y = -0.26807x + 3.7973	y = -0.27944x + 3.8635	y = -0.26807x + 3.8341	y = -0.28146x + 3.9175
Derived fatigue limit (MPa)	86.363	85.662	100.343	98.077	109.234	107.641
Fitted fatigue limit (MPa)	87.641	87.641	98.880	98.80	106.768	106.768
Error (%)	-1.458	-2.258	1.479	-0.812	2.310	0.818

5. Results and discussion

In this study, through fatigue tests and finite element simulations of spot-welded joints, the normalized *S-N* curve of spot-welded joints was studied based on the structural stress method, and a method for predicting the *S-N* curve was proposed. The following conclusions were drawn.

The correlation of the $\triangle F$-*N* curves of the spot-welded joints was weak, and the materials had a significant influence on the curves. When predicting the fatigue life of the spot-welded joints with different materials, fatigue tests had to be performed for each structure; therefore, the $\triangle F$-*N* curves were non-universal.

The stress of the spot-welded joint can be easily obtained by extracting the force and moment of the beam-element nodes in the spot-welded shell-element model. Using the equivalent-structural-stress calculation model, the equivalent structural stress of the spot-welded joint can be accurately obtained.

The correlation of the *S-N* curves of the spot-welded joints of the same material was satisfactory, and the correlation of the *S-N* curves of different materials was weak. Therefore, the material has a significant influence on the *S-N* curves, and the influence of materials cannot be ignored in the fatigue analysis of spot-welded joints.

To avoid the influence of materials on the *S-N* curves of spot-welded joints, a method for predicting the *S-N* curve was proposed based on the relationship between the ratio of the tensile strength and that of the fatigue limit of each material, which provides references for the design of spot-welding structures and life prediction in engineering applications.

Owing to the limitations of the test conditions and the amount of available test data, some data were dispersive and did not provide accurate solutions; therefore, supplementary tests should be conducted to improve the accuracy of the results. In the future, the influence of residual stress on the fatigue life and fatigue characteristics of spot-welded joints under tensile loads can be further investigated.

Acknowledgement

The authors are grateful for the financial support provided by the the National Natural Science Foundation of China (grant number 52175123) and the Independent Subject of State Key Laboratory of Traction Power (grant number 2022TPL_T03).

References

[1] Yang, L., Yang, B., Yang, G.W., Xiao, S.N., Zhu, T., Wang, F. (2020). S-N curve and quantitative relationship of single-spot and multi-spot weldings, *International Journal of Simulation Modelling*, Vol. 19, No. 3, 482-493, doi: 10.2507/IJSIMM19-3-CO11.

[2] Wang, F. (2018). *Research on equivalent stress method of spot welding and ring welding*, Master Thesis, Southwest Jiaotong University, Chengdu, China.

[3] Ismail, M.I.S., Afieq, W.M. (2016). Thermal analysis on a weld joint of aluminium alloy in gas metal arc welding, *Advances in Production Engineering & Management*, Vol. 11, No. 1, 29-37, doi: 10.14743/apem2016.1.207.

[4] Talabi, S.I., Owolabi, O.B., Adebisi, J.A., Yahaya, T. (2014). Effect of welding variables on mechanical properties of low carbon steel welded joint, *Advances in Production Engineering & Management*, Vol. 9, No. 4, 181-186, doi: 10.14743/apem2014.4.186.

[5] Dunder, D., Samardzic, I., Simunovic, G., Konjatic, P. (2020). Steel weldability investigation by single and double-pass weld thermal cycle simulation, *International Journal of Simulation Modelling*, Vol. 19, No. 2, 209-218, doi: 10.2507/IJSIMM19-2-510.
[6] Edwin Raja Dhas, J. Kumanan, S. (2013). Modeling and prediction of HAZ using finite element and neural network modeling, *Advances in Production Engineering & Management*, Vol. 8, No. 1, 13-24, doi: 10.14743/ apem2013.1.149.
[7] ISO 14324-2003. Resistance spot welding – Destructive tests of welds – Method for the fatigue testing of spot welded joints, from *https://www.iso.org/standard/24088.html*, accessed January 6, 2022.
[8] NF A89-571-2004. Resistance spot welding – Destructive tests of welds – Method for the fatigue testing of spot welded joints, from *https://www.antpedia.com/standard/573005.html*, accessed January 5, 2022.
[9] JIS Z3138-1989. Method of fatigue testing for spot welded joint, from *https://www.docin.com/p-323321200.html*, accessed January 5, 2022.
[10] KS B 0528-2001. Resistance spot welding-Destructive tests of welds – Methods for the fatigue testing of spot welded joints, from *https://www.antpedia.com/standard/7006344-1.html*, accessed January 4, 2022.
[11] GB/T 15111-1994. Test method for shear tensile fatigue of spot welded joints, from *http://www.doc88.com/p-1478459027386.html*, accessed January 3, 2022.
[12] Wang, R.J., Shang, D.G., Shen, T., Yan, C.L. (2006). A review on fatigue life prediction approaches for spot-welded joint, *Mechanics in Engineering*, Vol. 28, No. 3, 9-14, doi: 10.3969/j.issn.1000-0879.2006.03.002.
[13] Radaj, D., Zhang, S. (1991). Stress intensity factors for spot welds between plates of unequal thickness, *Engineering Fracture Mechanics*, Vol. 39, No. 2, 391-413, doi: 10.1016/0013-7944(91)90053-4.
[14] Rupp, A., Störzel, K., Grubisic, V. (1995). Computer aided dimensioning of spot-welded automotive structures, *SAE Technical Paper 950711,* doi: 10.4271/950711.
[15] Sheppard, S.D. (1993). Estimation of fatigue propagation life in resistance spot welds, *Advances in Fatigue Predictive Techniques*, ASTM STP 1211, Vol. 2, 169-185, doi: 10.1520/STP15085S.
[16] Kang, H.T. (2007). Fatigue prediction of spot welded joints using equivalent structural stress, *Materials & Design*, Vol. 28, No. 3, 837-843, doi: 10.1016/j.matdes.2005.11.001.
[17] Dong, P. (2001). A structural stress definition and numerical implementation for fatigue analysis of welded joints, *International Journal of Fatigue*, Vol. 23, No. 10, 865-876, doi: 10.1016/S0142-1123(01)00055-X.
[18] Yan, K. (2015). *Fatigue strength analysis of tensile-shear spot weld specimen based on structural stress*, Kunming University of Science and Technology, Kunming, China.
[19] Yang, L., Yang, B., Yang, G., Xiao, S., Zhu, T. (2020). Overview of fatigue research of spot welded joints, *Journal of Mechanical Engineering*, Vol. 56, No. 14, 26-43, doi: 10.3901/JME.2020.14.026.
[20] Wu, X. (2016). *Study on fatigue testing and life prediction method of spot welded joints of steel*, Chongqing University, Chongqing, China.
[21] Yang, L., Yang, B., Yang, G., Xiao, S., Zhu, T., Wang, F. (2020). Analysis on fatigue characteristics of spot welded joints of stainless steel car body, *Transactions of the China Welding Institution*, Vol. 41, No. 7, 18-24, doi: 10.12073/j.hjxb.20191204005.
[22] Yang, G., Che, C., Yang, B., Zhu, T., Wang, F., Wang, J. (2019). Optimization research on S-N curve of ring welding structure based on structural stress method, *Fatigue & Fracture of Engineering Materials & Structures*, Vol. 42, No. 10, 2207-2219, doi: 10.1111/ffe.13023.
[23] Kang, H.-T., Wu, X., Khosrovaneh, A., Li, Z. (2017). Data processing procedure for fatigue life prediction of spot-welded joints using a structural stress method, In: Harlow, G., McKeighan, P., Nikbin, K., Wei , Z. (eds.), *Fatigue and Fracture Test Planning*, *Test Data Acquisitions and Analysis*, Vol. 1598, 198-211, doi: 10.1520/ STP159820 160054.
[24] BS EN 1999-1-3:2007. Eurocode 9: Design of aluminium structures-Part 1-3: Structures susceptible to fatigue, from *http://www.doc88.com/p-1106362384048.html*, accessed January 4, 2022.
[25] Luo, S., Liu, M., Zheng, X. (2020). Characteristics and life expression of fatigue fracture of G105 and S135 drill pipe steels for API grade, *Engineering Failure Analysis*, Vol. 116, Article No. 104705, doi: 10.1016/ j.engfailanal. 2020.104705.